# Change-point detection for recursive Bayesian geoacoustic inversions

Bien Aik Tan,[a] Peter Gerstoft, Caglar Yardim, and William S. Hodgkiss
*Marine Physical Laboratory, Scripps Institution of Oceanography, University of California San Diego, 9500 Gilman Drive, La Jolla, California 92093-0238*

(Received 27 August 2014; revised 16 March 2015; accepted 23 March 2015)

In order to carry out geoacoustic inversion in low signal-to-noise ratio (SNR) conditions, extended duration observations coupled with source and/or receiver motion may be necessary. As a result, change in the underlying model parameters due to time or space is anticipated. In this paper, an inversion method is proposed for cases when the model parameters change abruptly or slowly. A model parameter change-point detection method is developed to detect the change in the model parameters using the importance samples and corresponding weights that are already available from the recursive Bayesian inversion. If the model parameters change abruptly, a change-point will be detected and the inversion will restart with the pulse measurement after the change-point. If the model parameters change gradually, the inversion (based on constant model parameters) may proceed until the accumulated model parameter mismatch is significant and triggers the detection of a change-point. These change-point detections form the heuristics for controlling the coherent integration time in recursive Bayesian inversion. The method is demonstrated in simulation with parameters corresponding to the low SNR, 100–900 Hz linear frequency modulation pulses observed in the Shallow Water 2006 experiment [Tan, Gerstoft, Yardim, and Hodgkiss, J. Acoust. Soc. Am. **136**, 1187–1198 (2014)].
 [http://dx.doi.org/10.1121/1.4916887]

[ZHM] Pages: 1962–1970

## I. INTRODUCTION

In geoacoustic inversion, the underlying model parameters typically are assumed constant over the observation interval. Specifically, in the case of low signal-to-noise ratio (SNR), long-time coherent integration and source and/or receiver motion may lead to change in the environment over time or space. Therefore, a data-driven approach is needed for determining the appropriate coherent integration interval over which the underlying model parameters can be considered constant. One solution is to use change-point detection to control the coherent observation interval. Change-point detection can be used for a number of cases in ocean acoustics, for example:

(1) when tracking a ship with constant radial speed and detecting the point where it changes speed;
(2) when accumulating snapshots for beamforming weak targets, and the direction of arrival changes;
(3) when the underlying environmental parameters changes in geoacoustic inversion (the focus in this paper).

At the change-point, we need to stop and restart the data accumulation process.

A change-point is defined as the time when the underlying model parameters of sequential data have changed.[1–6] Here, abrupt and gradual change in the underlying model parameters is considered. When a change-point is detected, the current inversion concludes and a new inversion is started using post-change-point measurements. Methods for detecting abrupt model parameter change are well established using the Bayesian approach and consist of offline/retrospective[1,2] and online change-point methods.[3–6] Offline/retrospective change-point methods determine if a change-point has occurred at time index, $t < l$, for $l$ measurements, whereas online change-point methods only determine if a change-point has occurred at the $l$th time index.

Online change-point detection methods calculate the posterior probability density of the change-point at each time step incrementally as data arrives.[3–6] Most of these online change-point detection methods[3,5,6] adopt the particle filtering approach. The particles represent possible change-points and they are not the same as the particles in sequential geoacoustic inversions.[7] A majority of the change-point detection approaches either treat the auxiliary model parameters (parameters not under test) as known or as nuisance parameters that eventually will be integrated out analytically.[2–5] To integrate out nuisance parameters analytically, most approaches usually assume Gaussian distributed linear models[3–6] and change-point prior densities. The advantage is that the posterior density is Gaussian distribution, which can easily be integrated analytically. However, Gaussian distributed linear models are not appropriate in most geoacoustic inversion problems due to the non-linear relationship between model parameters and measurements.

Due to the low SNR nature of the observations and the non-linear model of the geoacoustic inversion application, offline/retrospective methods[1,2] are selected here for detecting change-points (see Sec. II C). The offline/retrospective methods accumulate observations before making a decision retrospectively that a change-point has occurred. Given a set of observations, offline/retrospective methods calculate the probabilities or likelihoods of all possible change-points. This is repeated when a new observation becomes available.

[a]Author to whom correspondence should be addressed. Electronic mail: btan@ucsd.edu

Coincidentally, detecting a change-point retrospectively can be done efficiently using the importance samples and corresponding weights that already are available naturally as a consequence of implementing the Bayesian inversion recursively.[8]

Methods for detecting gradual model parameter change are less developed and often require strong parametric assumption. For example, time-varying source-receiver separation can be reparameterized into initial source-receiver separation, initial source and receiver velocities and constant source and receiver accelerations.[8,9] However, reparameterizing all of the model parameters in the inversion will adversely increase the dimension of the parameter search space. A typical treatment of gradual model parameters change is applying sequential geoacoustic inversion or particle filtering to track the parameter posterior density between relatively short-interval measurements.[7,10,11] In low SNR conditions, the shorter-interval measurements will give undesirably lower likelihoods and higher parameter uncertainties. Alternatively, the change-point method for abrupt change can be used for the gradual change case. If the model parameters change gradually, the inversion (based on constant model parameters) may proceed to estimate an "average" value of the parameters until the accumulated model parameter mismatch error is significant and triggers the detection of a change-point. As shown later in Sec. III, change-point detection will help maximize the measurement interval to reduce parameter estimation uncertainty without significantly introducing bias in the estimation that is due to model mismatch.

These change-point detections form the heuristics for controlling the coherent integration time in recursive Bayesian inversion (see Sec. II). For simplicity in developing the change-point detection approach, a range-independent source-receiver environment is assumed with motion of both in the perpendicular dimension as shown in Fig. 1. In this paper, detecting change in the underlying model parameters is the main focus. Abrupt or gradual change of the environment takes place in the direction of source-receiver motion. Change-point detection will work for a real three-dimensional (3D) environment. This is because the environment used could be modeled as a two-dimensional (2D) range-dependent or 3D model where the actual direction of change is estimated. In Sec. III, the method is demonstrated in simulation with parameters corresponding to the low SNR, 100–900 Hz linear frequency modulation (LFM) pulses observed in the Shallow Water 2006 experiment. The change-point approach also could be applied to local matched-field geoacoustic inversions using towed arrays,[12–16] but this scenario is not considered here.

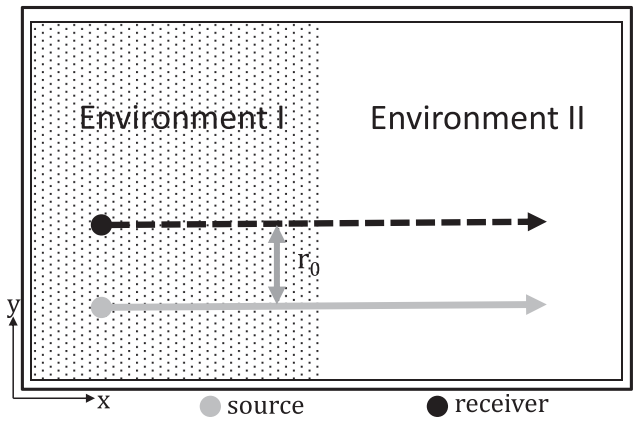


FIG. 1. Top view of the source-receiver trajectory schematics for change-point detection and recursive Bayesian inversion simulation. The source and receiver are assumed to move in the same direction and speed such that their relative velocity is zero.

## II. THEORY

Change-point models commonly are used to model discontinuity of model parameters or data over the length of the data. Given a sequence of observations, these models introduce a number of change-points that split the data into a set of disjoint segments. It, then, is assumed that the data arise from a single model within each segment, but with different models across the segments. For the recursive Bayesian inversion approach, the probability distributions (importance samples and weights) that are generated for model parameter estimates also can be used for inferences about the possible change-points.

Sections II A and II B first described the data model and recursive Bayesian inversion based on identical underlying model parameters.[8] Then, a single-change-point model is introduced where retrospective change-point detection is applied using Bayesian inference from the importance samples and weights from Sec. II B (see Sec. II C).

### A. Data model and likelihood function based on identical underlying model parameters

The source emits a sequence of identical pulses at a known repetition interval. The broadband data model for frequency-coherent matched field based geoacoustic inversion can be expressed as $L$ measurement vectors,[8]

$$\mathbf{y}_l = \mathbf{b}_l(\mathbf{m}) + \mathbf{g}_l, \tag{1}$$

where $\mathbf{y}_l = [y_l(\omega_{r1}) \cdots y_l(\omega_{rJ})]^T$ is the $K$-point fast Fourier transform (FFT) of the observed time series capturing the $l$th pulse for $J$ discrete frequencies. Note, the $l$th pulse Fourier transforms are synchronized to the first pulse transmission time $(t = 0)$. $\mathbf{m}$ is the subset of forward model parameters that are being estimated.

$\mathbf{b}_l(\mathbf{m}) = [\psi_l(\omega_{r1}, \mathbf{m}) \cdots \psi_l(\omega_{rJ}, \mathbf{m})]^T$ is the corresponding modeled or replica field generated using model vector, $\mathbf{m}$. It is assumed the model parameters, $\mathbf{m}$, do not change between measurements and, thus, the joint likelihood function will sharpen as $L$ increases.

The distribution of the error vector, $\mathbf{g}_l = [g_l(\omega_{r1}) \cdots g_l(\omega_{rJ})]^T$ defines the likelihood function. It is assumed that $\mathbf{g}_l$, for $l = 1, \ldots, L$, are independent and identically distributed (i.i.d.) across $L$ measurements. The frequency domain error vector, $\mathbf{g}_l$, is defined as complex Gaussian with mean, $\mathrm{E}[\mathbf{g}_l] = 0$, for $\omega_r \neq 0$ and autocovariance, $\mathbf{C}_\mathbf{g}$.[17]

The joint likelihood function of the $L$ measurements can be expressed as (based on i.i.d. measurements)

$$\mathcal{L}(\mathbf{m}) = p(\mathbf{y}_{1:L}|\mathbf{m}) = \prod_{l=1}^{L} p(\mathbf{y}_l|\mathbf{m}) = \prod_{l=1}^{L} \frac{1}{\pi^J |\mathbf{C_g}|} \times \exp\left\{ -[\mathbf{y}_l - \mathbf{b}_l(\mathbf{m})]^H \mathbf{C_g}^{-1} [\mathbf{y}_l - \mathbf{b}_l(\mathbf{m})] \right\}, \quad (2)$$

where supervector $\mathbf{y}_{1:L} = [\mathbf{y}_1^T, \ldots, \mathbf{y}_L^T]^T$.

### B. Recursive Bayesian estimation

Recursive Bayesian estimation is based on recursive Bayesian online learning[18] and on the importance sampling concept used in particle filter theory.[19–22] With initial prior knowledge of the parameters, $p(\mathbf{m})$, constant underlying model parameters, $\mathbf{m}$, and Bayes' rule, the joint posterior probability density function (posterior probability density, PPD) of the model parameters for $l$ pulse measurements is[18]

$$p(\mathbf{m}|\mathbf{y}_{1:l}) = \frac{p(\mathbf{y}_{1:l}|\mathbf{m})p(\mathbf{m})}{p(\mathbf{y}_{1:l})} \quad (3)$$

$$= \frac{p(\mathbf{y}_l|\mathbf{m})p(\mathbf{m}|\mathbf{y}_{1:(l-1)})}{\int p(\mathbf{y}_l|\mathbf{m})p(\mathbf{m}|\mathbf{y}_{1:(l-1)})\mathrm{d}\mathbf{m}}. \quad (4)$$

Equation (4) shows that the joint posterior density conditioned on $l$ measurements can be updated recursively from the $l$th likelihood and the joint posterior density of the $l-1$ measurements. Thus Bayesian updating of $p(\mathbf{m}|\mathbf{y}_{1:l})$ can be done all at once [Eq. (3)] or recursively over time [Eq. (4)]. In addition, assuming constant geoacoustic model parameters for all $l$, no model mismatch error, and no bias error between the replica and measured fields, the variance of the maximum *a posteriori* (MAP) parameter estimate,

$$\mathrm{var}[\hat{\mathbf{m}}_{\mathrm{MAP}}^{(L)}] < \mathrm{var}[\hat{\mathbf{m}}_{\mathrm{MAP}}^{(L-1)}] < \cdots < \mathrm{var}[\hat{\mathbf{m}}_{\mathrm{MAP}}^{(1)}], \quad (5)$$

where

$$\hat{\mathbf{m}}_{MAP}^{(L)} = \arg\max_{\mathbf{m}} p(\mathbf{m}|y_{1:L}) = \arg\max_{\mathbf{m}} p(\mathbf{m}) \prod_{l=1}^{L} p(y_l|\mathbf{m}). \quad (6)$$

Ideally, the posterior density converges to a Dirac delta function centered at the true parameter value as $L$ approaches infinity.[18] Practically, it is difficult to attain the true parameter value as there will be some model mismatch error or bias in the estimator. In addition, only a limited number of measurements can be processed before time-dependent variations in the model parameters and model mismatch errors become significant.

For this paper, the posterior density, $p(\mathbf{m}|\mathbf{y}_{1:l})$, is utilized to infer the possible change-points (see Sec. II C). The posterior density, $p(\mathbf{m}|\mathbf{y}_{1:l})$, can be represented by importance samples, $\{\mathbf{m}^q,\ q = 1, \ldots, Q\}$, that are drawn from the Gaussian mixture, $x(\mathbf{m}; l)$, in an adaptive importance sampling procedure described in detail in Ref. 8. From these importance samples, $\mathbf{m}^q$, the corresponding uncorrected and unnormalized weights, $\hat{w}_l^q$, were computed recursively using

$$\hat{w}_l^q = p(\mathbf{y}_{1:l}|\mathbf{m}^q)p(\mathbf{m}^q) = p(\mathbf{y}_l|\mathbf{m}^q)\hat{w}_{l-1}^q. \quad (7)$$

Because the importance samples are drawn from the Gaussian mixture, $x(\mathbf{m}; l)$, instead of the posterior density, $p(\mathbf{m}|\mathbf{y}_{1:l})$, the weights have to be corrected and normalized to represent the posterior density, $p(\mathbf{m}|\mathbf{y}_{1:l})$, correctly. The correction is

$$\tilde{w}_l^q = \hat{w}_l^q / x(\mathbf{m}^q; l). \quad (8)$$

Let normalized weights be $w_l^q = \tilde{w}_l^q / \sum_{j=1}^{j=Q} \tilde{w}_l^j$. The PPD can be approximated by[19,20]

$$p(\mathbf{m}|\mathbf{y}_{1:l}) \approx \sum_{q=1}^{Q} \delta(\mathbf{m} - \mathbf{m}^q) w_l^q, \quad (9)$$

and it approaches the true PPD as $Q \to \infty$.

### C. Change-point detection

We now consider the following class of single change-point models,[1] where the change-point may consist of change in one or several parameters. Let the sequence of non-overlapping measurement vectors be $\mathbf{y}_{1:L} = [\mathbf{y}_1^T, \ldots, \mathbf{y}_L^T]^T$, where the data observation model and likelihood function are summarized in Sec. II A. Each measurement vector is i.i.d. with likelihood $p(\mathbf{y}|\mathbf{m})$. This sequence of measurements is assumed to have a change-point at $r$ $(1 \le r \le l)$, where $\mathbf{y}_l \sim p(\mathbf{y}_l|\mathbf{m}_1)$, $\forall l = 1, \ldots, r$ and $\mathbf{y}_l \sim p(\mathbf{y}_l|\mathbf{m}_2)$, $\forall l = r+1, \ldots, L$

$$\mathbf{y}_l = \begin{cases} \mathbf{b}_l(\mathbf{m}_1) + \mathbf{g}_l, & \text{if } l = 1, \ldots, r. \\ \mathbf{b}_l(\mathbf{m}_2) + \mathbf{g}_l, & \text{if } l = r+1, \ldots, L. \end{cases} \quad (10)$$

$\mathbf{m}$ and $\mathbf{g}_l$ are the model parameters and noise, respectively, and $\mathbf{b}_l(\mathbf{m})$ is the transformation of the model parameters into the signal observed in the data, $\mathbf{y}_l$.

The joint likelihood of the $\mathbf{y}_{1:L}$ conditioned on $\mathbf{m}_1$ and $\mathbf{m}_2$ is[1]

$$p(\mathbf{y}_{1:L}|r, \mathbf{m}_1, \mathbf{m}_2) = p(\mathbf{y}_{1:r}|\mathbf{m}_1)p(\mathbf{y}_{r+1:L}|\mathbf{m}_2) = \prod_{l=1}^{r} p(\mathbf{y}_l|\mathbf{m}_1) \prod_{l=r+1}^{L} p(\mathbf{y}_l|\mathbf{m}_2). \quad (11)$$

The change-point is assumed to have prior density, $p(r)$, such that $\sum_{r=1}^{L} p(r) = 1$. Using Bayes rule, the PPD of the possible change-points, conditioned on all the measurements, is[1]

$$p(r|\mathbf{y}_{1:L}) \propto p(\mathbf{y}_{1:L}|r)p(r), \quad (12)$$

where

$$p(\mathbf{y}_{1:L}|r) = \int p(\mathbf{y}_{1:L}|r, \mathbf{m}_1, \mathbf{m}_2)p(\mathbf{m}_1, \mathbf{m}_2)\mathrm{d}\mathbf{m}_1\mathrm{d}\mathbf{m}_2 = \int p(\mathbf{y}_{1:r}|r, \mathbf{m}_1)p(\mathbf{m}_1)\mathrm{d}\mathbf{m}_1 \times \int p(\mathbf{y}_{r+1:L}|r, \mathbf{m}_2)p(\mathbf{m}_2)\mathrm{d}\mathbf{m}_2. \quad (13)$$

It also is assumed that the model parameters before and after the change-point are independent.[3,4] Equations (12) and (13) can be evaluated via Monte Carlo integration using the importance samples from the recursive Bayesian inversion.

Here, we further assume a uniform prior for the change-point. The maximum likelihood estimate of the change-point is

$$\hat{r} = \arg\max_{r} p(\mathbf{y}_{1:r}|\hat{\mathbf{m}}_{1,r})p(\mathbf{y}_{r+1:L}|\hat{\mathbf{m}}_{2,r}), \tag{14}$$

where

$$\hat{\mathbf{m}}_{1,r} = \arg\max_{\mathbf{m}} p(\mathbf{m}|\mathbf{y}_{1:r}), \tag{15}$$

and

$$\hat{\mathbf{m}}_{2,r} = \arg\max_{\mathbf{m}} p(\mathbf{m}|\mathbf{y}_{r+1:L}) \tag{16}$$

are the MAP estimates of the model parameters, $\mathbf{m}_1$ and $\mathbf{m}_2$, conditioned on the measurements prior to and after the hypothesize change-point, $r$, respectively. Equation (14) yields a significant peak only if a change-point is present in the measurements. If there is no underlying change-point in the measurements collected, then Eq. (14) will be equally likely for all hypothesized $r$. To determine the presence of a change-point, a normalized log-likelihood,

$$\mathcal{L}(r) = 10\ \log_{10}\frac{p(\mathbf{y}_{1:r}|\hat{\mathbf{m}}_{1,r})p(\mathbf{y}_{r+1:L}|\hat{\mathbf{m}}_{2,r})}{\max_{r} p(\mathbf{y}_{1:r}|\hat{\mathbf{m}}_{1,r})p(\mathbf{y}_{r+1:L}|\hat{\mathbf{m}}_{2,r})}, \tag{17}$$

is used and if $\max\max \mathcal{L}(r) - \min \mathcal{L}(r) \geq \beta$, then a change-point is detected. $\beta$ is a threshold determined by trial and error. Here, a change-point is detected if the maximum likelihood is ten times higher than the minimum likelihood, which means $\beta$ is set to 10 dB.

In Sec. II B, the importance samples and their associated uncorrected and unnormalized weights, $\{\mathbf{m}^q, \hat{w}_l^q\}$, where $\hat{w}_l^q = p(\mathbf{y}_{1:l}|\tilde{\mathbf{m}}^q)p(\tilde{\mathbf{m}}^q)$ were computed recursively using $\hat{w}_l^q = p(\mathbf{y}_l|\tilde{\mathbf{m}}^q)\hat{w}_{l-1}^q$. Note that $\mathbf{m}^q$ are drawn from a Gaussian mixture. Using these weights, the posterior density is obtained from

$$p(\mathbf{m}|\mathbf{y}_{1:r}) \approx \sum_{q=1}^{Q} \delta(\mathbf{m} - \mathbf{m}^q)\frac{\hat{w}_r^q}{x(\mathbf{m}^q; L)}, \tag{18}$$

and

$$p(\mathbf{m}|\mathbf{y}_{r+1:L}) \approx \sum_{q=1}^{Q} \delta(\mathbf{m} - \mathbf{m}^q)\frac{\hat{w}_L^q p(\mathbf{m}^q)}{\hat{w}_r^q x(\mathbf{m}^q; L)}, \tag{19}$$

where the weights, $\hat{w}_l^q$, correspond to the $Q$ importance samples.

The likelihoods also are inferred using the weights in the recursive Bayesian inversion from

$$p(\mathbf{y}_{1:r}|r, \mathbf{m}^q) = \frac{\hat{w}_r^q}{p(\mathbf{m}^q)} \tag{20}$$

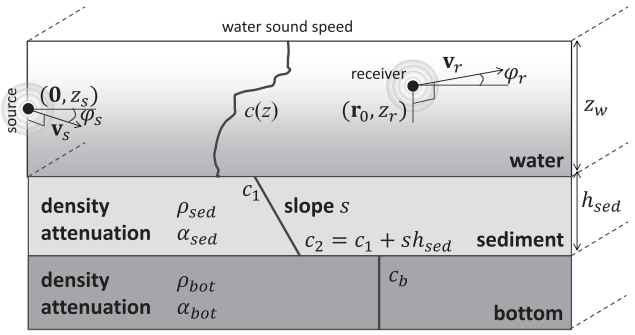


FIG. 2. Horizontally stratified ocean with a horizontally moving source and receiver. The source is moving at velocity, $\mathbf{v}_s$, and bearing, $\varphi_s$, while the receiver is moving at velocity, $\mathbf{v}_r$, and bearing, $\varphi_r$. The range origin is the source position at time zero when the source begins transmitting.

and

$$p(\mathbf{y}_{r+1:L}|r, \mathbf{m}^q) = \frac{\hat{w}_L^q}{\hat{w}_r^q}. \tag{21}$$

Therefore, change-point detection, computationally, is convenient when used with the recursive Bayesian inversion. By re-using the weights from the recursive Bayesian inversion, there is no need to recompute likelihoods and posterior densities explicitly.

## III. SIMULATION

This section will demonstrate change-point detection in abrupt and gradual model parameter change. Upon detection, the current recursive Bayesian inversion will conclude and a new inversion will begin. The ocean model is illustrated in Fig. 2 and model parameters are tabulated in Table I. Based on the theory presented in Sec. II, this simulation models a source and receiver moving in the same direction as the horizontal x-axis and at the same speed of 2 m/s for $L = [1, \ldots, 128]$ pulses (see Fig. 3). The source and receiver are assumed to be separated in distance by $r_0$ in the $y$ direction as depicted in Fig. 3. Hence, the relative source-receiver velocity is equal to zero.

TABLE I. Baseline model parameters.

| Simulation model parameters | Value |
|---|---|
| Source-receiver separation at $t = 0$, $r_0$ (m) | 600 |
| Source depth, $z_s$ (m) | 30 |
| Receiver depth, $z_r$ (m) | 45 |
| Source radial velocity, $v_s$ (m/s) | 0 |
| Receiver radial velocity, $v_r$ (m/s) | 0 |
| Water depth, $z_w$ (m) | 78 |
| Sediment depth, $h_{\text{sed}}$ (m) | 22 |
| Sediment density, $\rho_{\text{sed}}$ (g/cm$^3$) | 1.8 |
| Sediment attenuation, $\alpha_{\text{sed}}$ (dB/$\lambda$) | 0.2 |
| Sediment top velocity, $c_1$ (m/s) | 1640 |
| Sediment velocity slope, $s$ (1/s) | 0 |
| Bottom density, $\rho_{\text{bot}}$ (g/cm$^3$) | 2.2 |
| Bottom attenuation, $\alpha_{\text{bot}}$ (dB/$\lambda$) | 0.2 |
| Bottom velocity, $c_b$ (m/s) | 1740 |

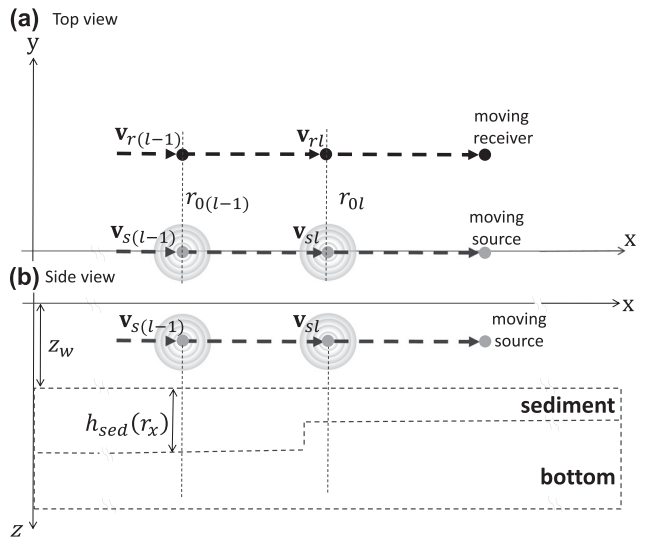


FIG. 3. $x$ and $y$ are the horizontal axes where the origin is the source position at time zero when the source begins transmitting. Source and receiver are moving in the same $x$ direction and at the same speed. The source-receiver separation is constant and the geoacoustic properties are assumed range-independent in the $y$ direction. Shown above are the source and receiver positions just prior and after the abrupt change in sediment thickness. (a) Top view. (b) Side view.

The environment is assumed range independent between the source and receiver while range dependent along the source or receiver track. The range-independent geoacoustic parameters were based on previous SW06 inversion results.[8,9,23–26] The source emits 100–900 Hz LFM pulses with 1 s pulse width and 5 s pulse repetition interval. Hence, for $l = 128$, the source and receiver would have traversed $5 \times 128 \times 2 = 1280$ m. The frequency sampling is 5 Hz starting from 100 Hz to 700 Hz. KRAKEN is used to compute the modes and wavenumbers.[27]

The suggested change-point detection scheme is applicable to change in one or several parameters. In Fig. 4, the objective is to simulate and detect an abrupt change in the sediment thickness along the track in recursive Bayesian inversion. The true sediment thickness, $h_{\text{sed}}$, is fixed at 22 m for $l = 1$ to $l = 64$ and then fixed at 17 m for $l = 65$ to $l = 128$ to simulate an abrupt change in sediment thickness, $h_{\text{sed}}$. The sediment parameters ($h_{\text{sed}}$, $c_1$, $s$, and $\alpha_{\text{sed}}$) are estimated using the recursive Bayesian estimation procedure, while the rest of the model parameters are assumed known. In addition, the weights from the inversion are being used for change-point detection detailed in Sec. II. In Fig. 4, only

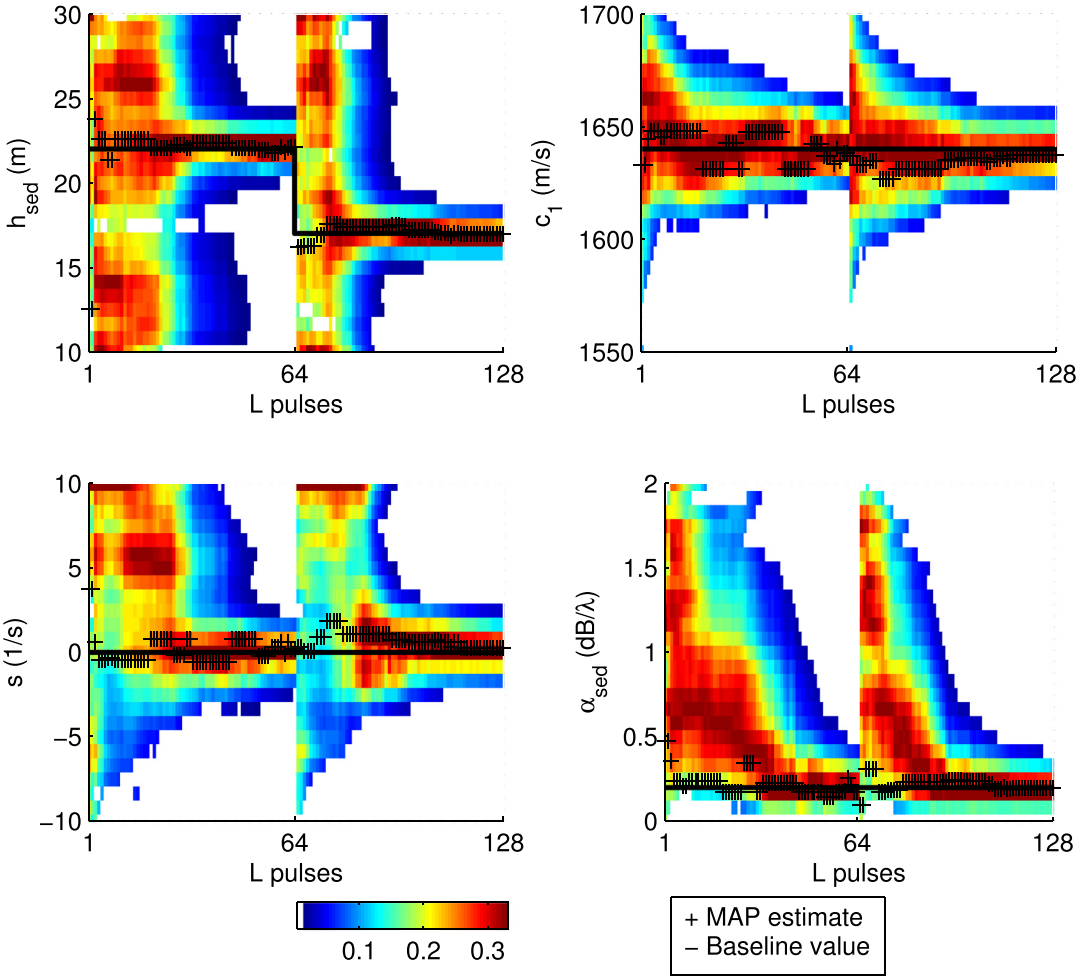


FIG. 4. (Color online) Evolution of 1-D marginal PPD with SNR fixed at 0 dB, and number of LFM pulses $L = 1-128$ with change-point detected at $r = 64$. Only the 95% highest posterior density (HPD) portion (non-white) PPD is plotted. When a change-point is detected, the inversion restarts and the post-change-point PPD and MAP estimates are based on $L - r$ pulses measurement, where $r$ is the most recent change-point.

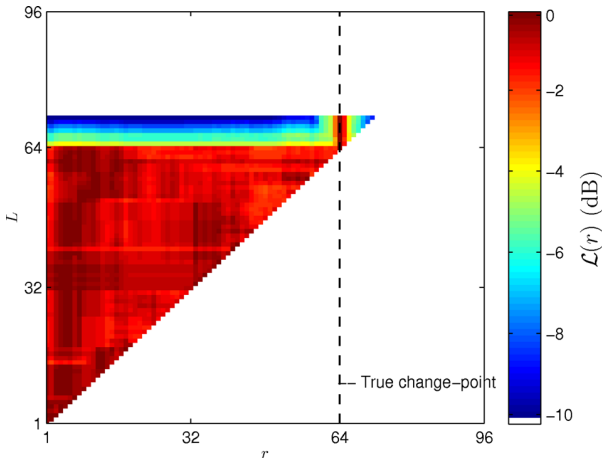


FIG. 5. (Color online) Evolution of change-point likelihood, $L$, with SNR fixed at 0 dB, and number of LFM pulses $L = 1{-}71$ with change-point detected ($\beta = 10$ dB) at $r = 64$ and $L = 71$.

the 95% highest posterior density (HPD) regions[28,29] of the one-dimensional (1D) marginal PPD and MAP parameter estimates for each model parameter are reconstructed based on $L - r$ pulse measurements, where $r$ is the most recent change-point. The change-point is detected correctly at $r = 64$ and the current inversion concludes based on $l = 1 : r$ pulse measurements. A new inversion is started using post-change-point $r + 1$th pulse measurement onward and, hence, the sudden increase in uncertainties at $L = 64$.

Not shown in Fig. 4 is the number of post-change-point measurements needed for a change-point to be detected retrospectively. In Fig. 5, the time-evolving change-point log-likelihood, $\mathcal{L}(r)$, is plotted for $L = 1{-}71$. It is noted the change-point log-likelihood is equally likely when a change-point is absent ($L < 64$). However, when a change-point is present, a peak at $r = 64$ emerges as more post-change-point measurements are collected. Finally, a change-point is detected at $r = 64$ when $L = 71$ (threshold $\beta = 10$ dB). At this stage, only the pre-change-point importance samples are retained, while the post-change-point importance samples are discarded. It is expected that a multiple parameter change-point will have a relatively larger mismatch error than a single parameter change-point. As such, less post-change-point measurements are required for triggering the change-point detection.

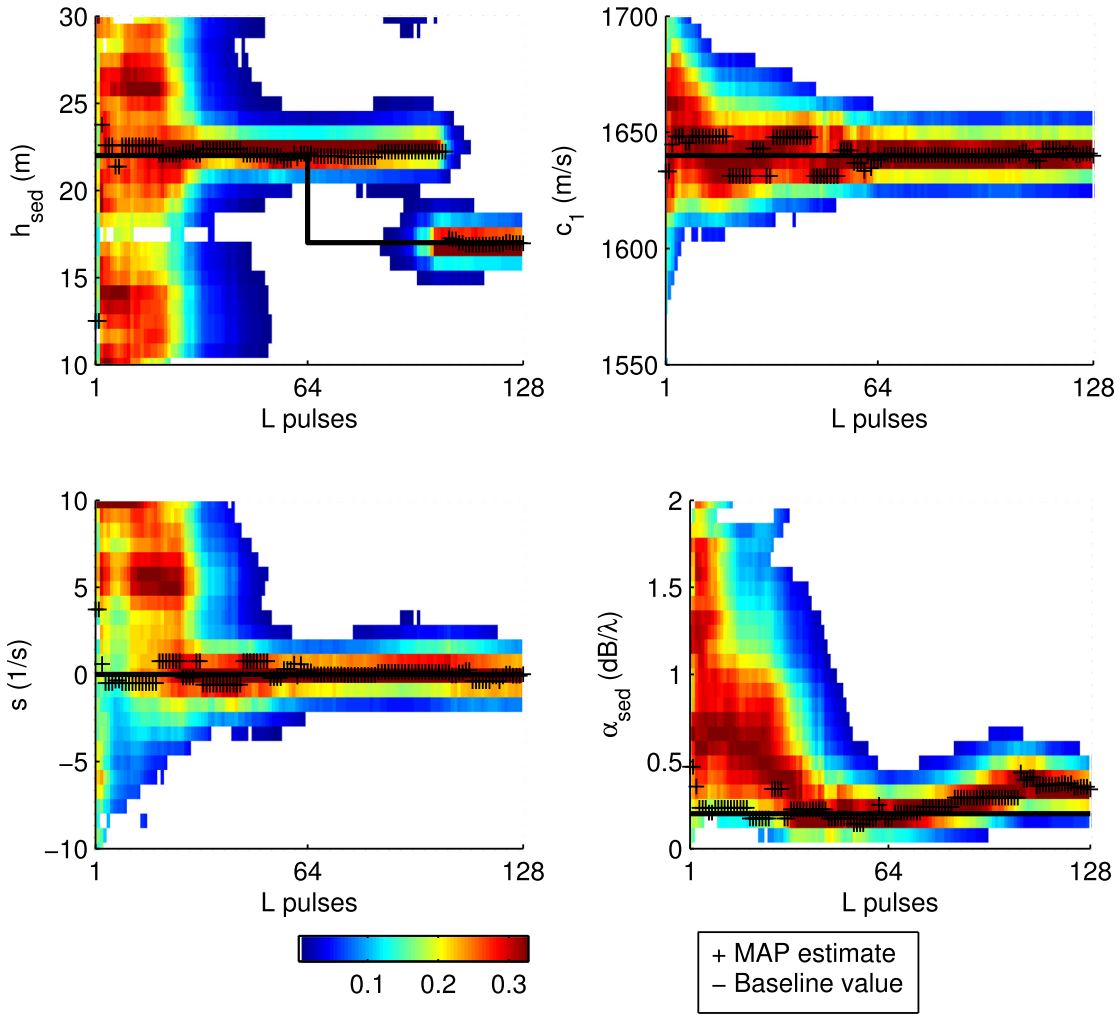


FIG. 6. (Color online) Evolution of 1-D marginal PPD with SNR fixed at 0 dB, and number of LFM pulses $L = 1{-}128$ without change-point detection. The inversion (based on constant model parameters) is allowed to proceed despite an abrupt change at $L = 64$ in the sediment thickness. Only the 95% HPD portion (non-white) PPD is plotted.

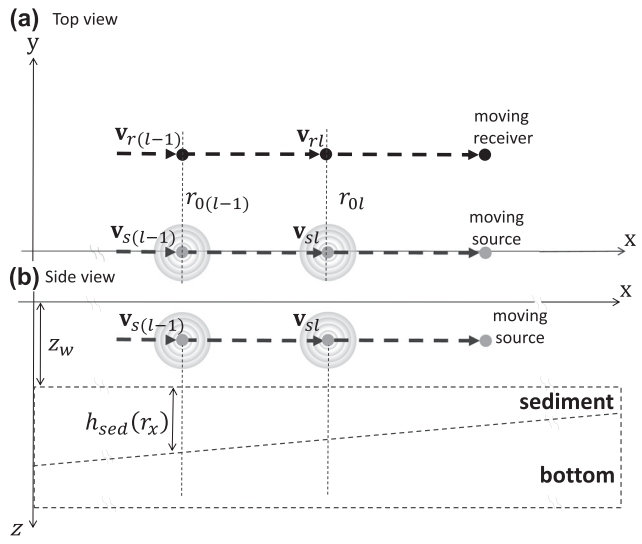


FIG. 7. $x$ and $y$ are the horizontal axes where the origin is the source position at time zero when the source begins transmitting. Source and receiver are moving in the same $x$ direction and at the same speed. The source-receiver separation is constant and the geoacoustic properties are assumed range independent in the $y$ direction. Shown above are the source and receiver positions in the midst of gradual change in sediment thickness.

The simulation is repeated with no change-point detection. Hence, the inversion (based on constant model parameters) is allowed to proceed despite an abrupt change in the sediment thickness at $L = 64$ (see Fig. 6). Due to the model mismatch error, the inversion results for $L > 64$ are biased (see $h_{\text{sed}}$ and $\alpha_{\text{sed}}$).

Next, a gradual change (from 22 m to 17 m) in the sediment thickness is simulated (see Figs. 7 and 8). When the accumulated model mismatched error is significant, a change-point detection is triggered. Here, two change-points have been triggered at $L = 41$ and $L = 71$. Despite the model mismatch in fitting a constant parameter model to a gradual change parameter model, there is no significant bias in the MAP estimates. The MAP estimates for the sediment thickness converge to an "average" value between the minimum and maximum values for each segment. Here, the gradually changing parameter model is segmented via the change-point detection method into three models, each with a different set of constant parameters.

Figure 9 shows the time-evolving change-point log-likelihood, $\mathcal{L}(r)$, for $L = 1-63$. There are two differences when comparing Figs. 6 and 9. First, the change-point likelihood is less peaky across $r$ in the gradual change case. This

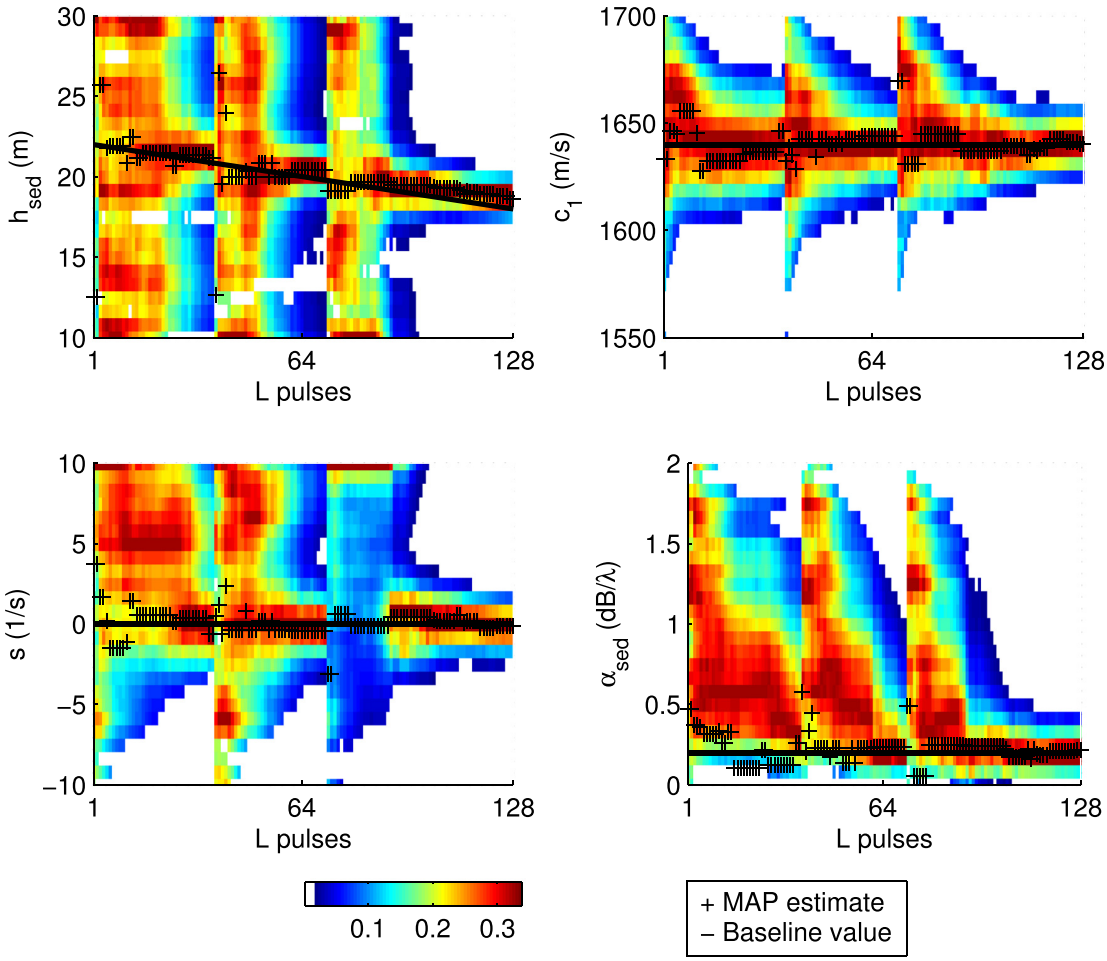


FIG. 8. (Color online) Evolution of 1-D marginal PPD with SNR fixed at 0 dB, and number of LFM pulses $L = 1-128$ with change-point detection. True sediment thickness changes gradually from 22 m to 17 m. Only the 95% HPD portion (non-white) PPD is plotted.

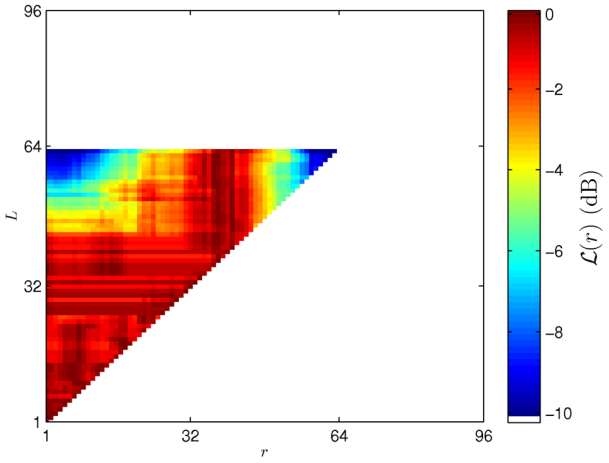


FIG. 9. (Color online) Evolution of change-point likelihood, $L$, with SNR fixed at 0 dB, and number of LFM pulses $L = 1-77$ with change-point detected on gradual change in $h_{\text{sed}}$ ($\beta = 10$ dB) at $r = 41$ and $L = 63$.

is expected as the method is designed for abrupt/non-gradual parameter change. Second, the number of post-change-point measurements is comparable to the number of pre-change-point measurements. This, also, is expected. Given a set of measurements derived from a model with a gradually changing parameter, bisecting the measurements is probably the best way to approximate the gradual parameter change with two constant models, $\mathbf{m}_1$, $\mathbf{m}_2$.

## IV. CONCLUSIONS

A key assumption for recursive Bayesian matched field geoacoustic inversions is constant underlying model parameters. When there is long-time coherent integration and source-receiver motion, change in the underlying model parameters due to time or space is anticipated. Modeling the change parametrically would be desirable, but also adversely increases the dimension of the inversion search space. Instead, a model parameter change-point detection method that detects abrupt or gradual change in model parameters can be utilized. Combining change-point detection and recursive Bayesian inversion has enabled a data-driven verification of the constant model parameter assumption. When a change-point is detected, the current inversion concludes and a new inversion is started using post-change-point measurements. This method was demonstrated in simulation with parameters corresponding to the Shallow Water 2006 experiment.

Note that a change-point detection will not indicate which model parameters have changed. In order to determine which specific model parameters have changed, the post-change-point detection inversion has to integrate over a sufficiently long interval to estimate the parameters well and compare them with the pre-change-point inversion. A potential extension of this method would be to determine which parameters have changed upon detection of a change-point and, then, use the posterior information from the pre-change-point inversion to assign an appropriate prior density to the post-change-point inversion.

## ACKNOWLEDGMENTS

This work was supported by the Office of Naval Research Grant No. N00014-11-0320 and the DSO National Laboratories of Singapore.

[1]A. F. M. Smith, "A Bayesian approach to inference about a change-point in a sequence of random variables," Biometrika **62**, 407–416 (1975).
[2]J. J. K. Ruanaidh and W. J. Fitzgerald, *Numerical Bayesian Methods Applied to Signal Processing* (Springer, New York, 1996), pp. 96–121.
[3]P. Fearnhead and Z. Liu, "On-line inference for multiple changepoint problems," J. R. Stat. Soc.: Ser. B **69**, 589–605 (2007).
[4]R. P. Adams and D. J. MacKay, "Bayesian online changepoint detection," http://hips.seas.harvard.edu/content/bayesian-online-changepoint-detection.
[5]J. Mellor and J. Shapiro, "Thompson sampling in switching environments with Bayesian online change detection," in *Proceedings of the Sixteenth International Conference on Artificial Intelligence and Statistics* (2013), pp. 442–450.
[6]F. Caron, A. Doucet, and R. Gottardo, "On-line changepoint detection and parameter estimation with application to genomic data," Statist. Comput. **22**, 579–595 (2012).
[7]C. Yardim, P. Gerstoft, and W. S. Hodgkiss, "Tracking of geoacoustic parameters using Kaman and particle filters," J. Acoust. Soc. Am. **125**, 746–760 (2009).
[8]B. A. Tan, P. Gerstoft, C. Yardim, and W. S. Hodgkiss, "Recursive Bayesian synthetic aperture geoacoustic inversion in the presence of motion dynamics," J. Acoust. Soc. Am. **136**, 1187–1198 (2014).
[9]B. A. Tan, P. Gerstoft, C. Yardim, and W. S. Hodgkiss, "Broadband synthetic aperture geoacoustic inversion," J. Acoust. Soc. Am. **134**, 312–322 (2013).
[10]C. Yardim, P. Gerstoft, and W. S. Hodgkiss, "Geoacoustic and source tracking using particle filtering: Experimental results," J. Acoust. Soc. Am. **128**, 75–87 (2010).
[11]C. Yardim, P. Gerstoft, and W. S. Hodgkiss, "Sequential geoacoustic inversion at the continental shelfbreak," J. Acoust. Soc. Am. **131**, 1722–1732 (2012).
[12]M. Siderius, P. L. Nielsen, and P. Gerstoft, "Range-dependent seabed characterization by inversion of acoustic data from a towed receiver array," J. Acoust. Soc. Am. **112**, 1523–1535 (2002).
[13]D. J. Battle, P. Gerstoft, W. A. Kuperman, W. S. Hodgkiss, and M. Siderius, "Geoacoustic inversion of tow-ship noise via near-field-matched-field processing," IEEE J. Oceanic Eng. **28**, 454–467 (2003).
[14]D. J. Battle, P. Gerstoft, W. S. Hodgkiss, W. A. Kuperman, and P. L. Nielsen, "Bayesian model selection applied to self-noise geoacoustic inversion," J. Acoust. Soc. Am. **116**, 2043–2056 (2004).
[15]J. Dettmer, S. E. Dosso, and C. W. Holland, "Sequential trans-dimensional Monte Carlo for range-dependent geoacoustic inversion," J. Acoust. Soc. Am. **129**, 1794–1806 (2011).
[16]J. Dettmer and S. E. Dosso, "Probabilistic two-dimensional water-column and seabed inversion with self-adapting parameterizations," J. Acoust. Soc. Am. **133**, 2612–2623 (2013).
[17]A. Papoulis and S. Pillai, *Probability, Random Variables, and Stochastic Processes*, 4th ed. (McGraw-Hill, New York, 2002), p. 515, 519.
[18]R. Duda, P. Hart, and D. Stork, *Pattern Classification*, 2nd ed. (Wiley, New York, 2001), pp. 97–98, 531–534.
[19]A. Doucet, S. Godsill, and C. Andrieu, "On sequential Monte Carlo sampling methods for Bayesian filtering," Stat. Comput. **10**, 197–208 (2000).
[20]B. Ristic, S. Arulampalam, and N. Gordon, *Beyond the Kalman Filter: Particle Filters for Tracking Applications* (Artech House, Boston, 2004), pp. 35–39.
[21]D. Lee and N. Chia, "A particle algorithm for sequential Bayesian parameter estimation and model selection," IEEE Trans. Signal Process. **50**, 326–336 (2002).
[22]C. Yardim, Z. H. Michalopoulou, and P. Gerstoft, "An overview of sequential Bayesian filtering in ocean acoustics," IEEE J. Oceanic Eng. **36**, 71–89 (2011).
[23]C.-F. Huang, P. Gerstoft, and W. S. Hodgkiss, "Effect of ocean sound speed uncertainty on matched-field geoacoustic inversion," J. Acoust. Soc. Am. **123**, EL162–EL168 (2008).

[24]Y.-M. Jiang and N. R. Chapman, "Bayesian geoacoustic inversion in a dynamic shallow water environment," J. Acoust. Soc. Am. **123**, EL155–EL161 (2008).
[25]J. W. Choi, P. H. Dahl, and J. A. Goff, "Observations of the R reflector and sediment interface reflection at the shallow water'06 central site," J. Acoust. Soc. Am. **124**, EL128–EL134 (2008).
[26]C. Park, W. Seong, P. Gerstoft, and W. S. Hodgkiss, "Geoacoustic inversion using backpropagation," IEEE J. Oceanic Eng. **35**, 722–731 (2010).
[27]M. B. Porter, "The KRAKEN normal mode program," SACLANTCEN Memo. SM-245, SACLANT Undersea Research Centre, La Spezia, Italy (1991), Chap. 2.
[28]C.-F. Huang, P. Gerstoft, and W. S. Hodgkiss, "Uncertainty analysis in matched-field geoacoustic inversions," J. Acoust. Soc. Am. **119**, 197–207 (2006).
[29]C. Yardim, P. Gerstoft, and W. S. Hodgkiss, "Statistical maritime radar duct estimation using hybrid genetic algorithm Markov Chain Monte Carlo method," Radio Sci. **42**, RS3014 (2007).